Cassini Stellar Reference Unit: performance test approach and results

Valerie C. Thomas and Randel C. Blue

Jet Propulsion Laboratory, California Institute of Technology
4800 Oak Grove Drive, Pasadena, California 91109

Dorico Procopio

Officine Galileo
Via A. Einstein 35, 50013 Campi Bisenzio (Florence), Italy

ABSTRACT

The Cassini Stellar Reference Unit (SRU) is the prime attitude determination sensor on the Cassini spacecraft. 1(must operate continuously and reliably during both the cruise and the Saturnian tour phases of the mission. in fact, accuracy requirements are most critical toward the end of the mission, during the four years of scientific observations at Saturn.

To ensure that the SRU will operate within specification for the entire mission, an extensive test program has been undertaken to characterize d ie SRU performance prior to launch and to quantify any expected performance degradation. Results from several complimentary test programs are presented and compared with prc-test performance predictions. Additionally, a unique approach is described for enabling closed-loop testing of the SRU with the other elements of the. Cassini Attitude and Articulation Control Subsystem (AACS) when no optical stimulation is available.

Keywords: star tracker, e.harg,c-coupled dc.vice, attitude sensor, centroid accuracy, noise equivalent angle

1. IN'1"RO1)UC'I'1ON

The Stellar Reference Unit is a CCD based star tracker which, with its associated software, will provide autonomous star identification over the full sky. During much of the Cassini mission, the SRU will be the single source of attitude information. Three-axis spacecraft attitude reference will be determined by frequent measurements of up to five. stars in the SRU field of view allowing the Inertial Reference Units (IRUs) to be powered off during the cruise phase of the flight.

Officine Galileo (OG) has been responsible for the detailed design, assembly and test of the SRU hardware using flight-qualified CCDs provided by JPL. During flight, the operation of the redundant SRUs is under control of the AACS Flight Computer (AFC) and JPL developed star identification and tracking software. J}'], also has the responsibility for integrating the SRU hardware and software within the Cassini AACS. Consequently, performance testing has been a combination of device level tests of the CCD conducted at JPL., SRU assembly level tests at OG using a star simulator and sky tests of the SRU Engineering Model (EM) at JPL's '1'able Mountain observatory ('l"MC)).

2. SRU OVERVIEW

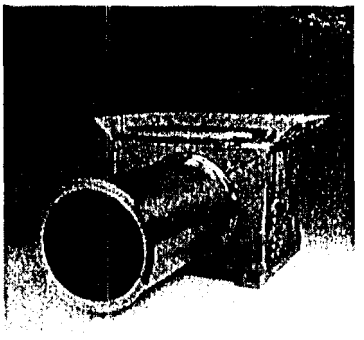

Fig. 1 Cassini SRU

The SRU, shown in Fig. 1, consists of a number of major elements. It contains a set of rcfr active optics, produced from radiation hard glass (Schott) and a Remote Terminal Input/Output Unit (RTIOU) interface board for receiving commands from and providing telemetry and status data to the AFC. SRU control logic, implemented in a custom ASIC, interprets commands received through the RTIOU and provides the necessary clock signals to drive the CCD and also monitors and controls the CCD temperature. Other elements of the SRU include a DC/DC convener, a high speed serial interface for transmitting digitized pixel data into AFC memory and a test interface called the Image Emulation Unit (IEU) interface. In addition, the SRU has a radiator for cooling the CCD to within its nominal operating temperature (-35 ± 5 °C) and a baffle. for attenuating signals and background light from bright sources outside the stray light FOV.

The SRU utilizes a 1024 x 1024, 3-phase, frontside-illuminated CCD with a 12 µm pixel sire. The CCD can be clocked in Multi-l) inned Phase (M PP) mode for dark current suppression and in anti-blooming mode for tracking with large objects (such as Saturn) or very bright stars in the FOV. Five stars can be tracked simultaneously with variable window sizes and integration times. On-chip charge summing, or pixel summation, can also be commanded when tracking at high rates or when fast acquisition is required, but image resolution is less critical.

Complete descriptions of the key design considerations and system trade-offs, as well as details of the SRU hardware implementation have. been published previously[1,2]. Table 1 provides a summary of the key requirements and characteristics of the SRU.

'f'able 1. SRU Performance Requirements and Characteristics

PARAMETER	REQUIREMENT
Accuracy, 3σ, pcr axis	65 µrad (1 star) 1 mrad twist (2 stars)
Sky Coverage	>99.5%
Sensitivity	$M_{vis} > 6$
Effective star temperature range	2500 to 10(X3O K
Number of stars hacked	Up to 5
Frame rate (commandable)	2-4 Hz (typical)
Pixel output data format	12 bit
FOV	150 (full cone angle)
Spectral bandwidth	550 to 770 nm (50% bandpass)
Optical coatings	Dichroic and anti-reflection
Straylight FOV	60 ° (full crmc angle)
Sun exposure	15 minutes at any angle, 0.6 - 9.0 AU
Mass	< 10 kg
Power	< 1 2 W
Lifetime	12 years in space., 2.5 years ground testing

3. TEST APPROACH AND RESULTS

The process of characterizing the expected performance of the SRU began with device level tests of the SRU CCDs. Information from these tests was then used by Officine Galileo in finalizing the design of the SRU, inducting selection of the appropriate CCD operating temperature, determination of the required amount of radiation shit.lcting and selection of the optimum device operating voltages. Officine Galileo then built an engineering model (EM) followed by three flight model SRUs. The] EM was initially tested by OG using a star simulator, but was eventually delivered [o J]', for real sky tests. Previous experience has shown that there is no substitute for real stars in testing out the capability of a star tracker. in this circumstance, it was also the first opportunity to operate a flight- like SRU with the actual Cassini star identification and tracking algorithms. The following sections describe these three intct-related test programs which ultimately led to the delivery of flight SRUs which arc expected to meet or exceed mission requirements.

3 . 1 CCD Performance Evaluation

Two general types of CCD-level evaluation were accomplished. First, qualification tests of sample parts from the flight lot were conducted to verify that the devices would function within specification during and after exposure to the expected launch arid flight environments. Vibration and the.r mal cycling of CCDs in flight packages had no effect on their performance. I1owcvcr, the natural space radiation environment and the radiation generated by the. RTGs carried on-board the spacecraft can cause. significant performance degradation of the CCD, so extensive radiation testing was also performed. Next, detailed device calibration tests of the flight candidate CCDs were meticulously undertaken to assess the unique operating characteristics of each individual part.

Sample dc.vices from the flight lot were exposed to 6 krad (Si) total radiation dose, which is three times the dose expected to be received during the mission. The radiation tests included gamma radiation ant] protons. The effects of the radiation on charge transfer efficiency (CTE), dark cur-rent spikes and dark current non-uniformity, dark current noise and ftat band shift were then evaluated. In summary:

(1) CTE degradation, while slightly higher than expected for the SRU devices, can, if necessary, be compensated for in the flight software and so is acceptable for this application.
(?) Flat hand shift, which can cause a decrease in pixel full well and an increase in dark current generation, was negligible.
(3) Dark current spikes affected approximately 0.02% of the device which is negligible when compared to the. 99.5% sky coverage requirement for the SRU. Dark current non-uniformity also only affected a small portion (appi oximately 2%) of the CCD and was readily absorbed within the SRU distortion error budget.
(4) The mean dark cur-rent rate increase was less than that assumed in developing the photometric budget so the end-of-life noise equivalent angle (NEA) is expected to be within the require.d specification.

Flight candidate parts, which had successfully completed initial screening and burn-in, were then subjected to a battery of tests to fully characterize their performance and to provide sufficient data for selection of the actual devices to be installed in the flight hardware. First, image maps were made to locate any cosmetic problems, such as dust or other particles located on the imaging surface. Histograms were made of the particle types, sires and percent light obscuration. Next, a set ics of tests were run to determine the set of operating voltages that optimized CTE, full well, linearity and read noise in each operating mode (MPP, partially inverted and anti-blooming). Once the.sc voltages were determined, full well, linearity, pixel summing and dark current measurements were taken using these baseline operating parameters. Additionally, a hot pixel map was generated and tests to investigate the device response to point source (star-like) illumination were conducted. Other tests, such as quantum efficiency and residual image tests, were performed using sample parts from the SRU lot, but not on each individual CCD. Fig. 2 is an example plot produced during the CCD characterization process showing full well measured as a function of positive parallel clock voltage.

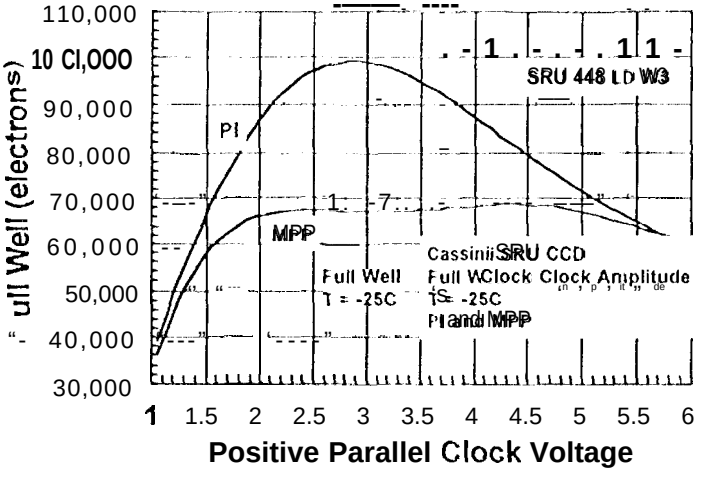

Fig. 2 Full Well Versus Positive Parallel Clock Voltage

Detailed device characterization was performed using the SRU clock wave forms with the detector cooled to SRU o])cr'sting temperatures. All the images, plots and other relevant data collected during the tests have been stored on tape and will be archived on CD-ROM for future reference.

3.2 Performance Verification Using a Star Simulator

The SRU per for mance has been extensively tested using a star simulator to verify the achievable accuracy using different star classes and under different environmental conditions (vibration and temperature). In this section, the test set-up used for per formance evaluation in the laboratory is described and the measured per formance is reported and compared with predicted rc.suits.

3.2.1 ASTRA Test Sa1-up

The pet formance tests were conducted at Officine Galileo using the ASTRA test facility. This system is composed of a star simulator and a two axis rotating table. The main system characteristics are:

Star simulator:

- Off axis parabolic mirror, focal length 2500 mm, high stability light source
- Beam diameter 250 mm, collimation <3 arcsec
- Filter wheels, for both neutral density and colored filters, to simulate different star magnitudes and colors
- Number of stars generate.(i: i

Rotating table:

- Resolution: 0.36 arcsec
- Accuracy (calibrated) over ± 8 degrees: ± 0.6 arcsec (worst case)
- Repeatability: O, 1 arcsec (short term)
- Capability to support a thermal chamber with -60 °C to + 90 °C temperature range

High accuracy positioning of the table is achieved by means of a laser interferometer system used to calibrate the raw error of the rotating table. The star simulator and the rotating table are mounted on a concrete basement and insulated from the ground with a vibration isolation system which increases the stability of the measurements. During data acquisition, the test chamber is maintained in darkness while the rotating table movements and SRU commanding and data processing are performed via remote computer control.

This test set up has been used extensively by Officine Galileo to verify the accuracy of the Infrared Space. Observatory (1S0), Solar and Heliospheric observatory (SOHO) anti Satellite Astronomia X-ray (SAX) star trackers. These star trackers have all frown successfully. Data collected in-flight has shown that the accuracy of the trackers was within 0,15 arcsec of the expected accuracy based on pre-flight, star simulator measurements.

During tests of the SRU, cooling of the CCD is achieved by removing the flight radiator and connecting the end of the thermal strap to a Support Cold Plate (SCP). The SCP is cooled by a thermoelectric cooling (TEC) system. To prevent frosting of cooled parts, the SRU, the SCP and the TEC are placed within in a vacuum container which is then mounted on the rotating table. The vacuum Container is provided with a quartz window [o allow optical stimulation of the unit under test. This configuration has the advantage that CCD cooling is achieved without moving parts. Vibrations introduced by the movement of the liquid flowing in the TEC heat sink are absorbed by the mass of the vacuum container, allowing high stability of the CCD during data acquisition. Moreover, the optics is under vacuum, so no air to vacuu III compensation is needed in the star simulator optical path.

A schematic of the SRU configuration inside the vacuum container is shown in Fig.3. The entire vacuum container can also be covered by a thermal chamber to verify measurement accuracy over temperature.

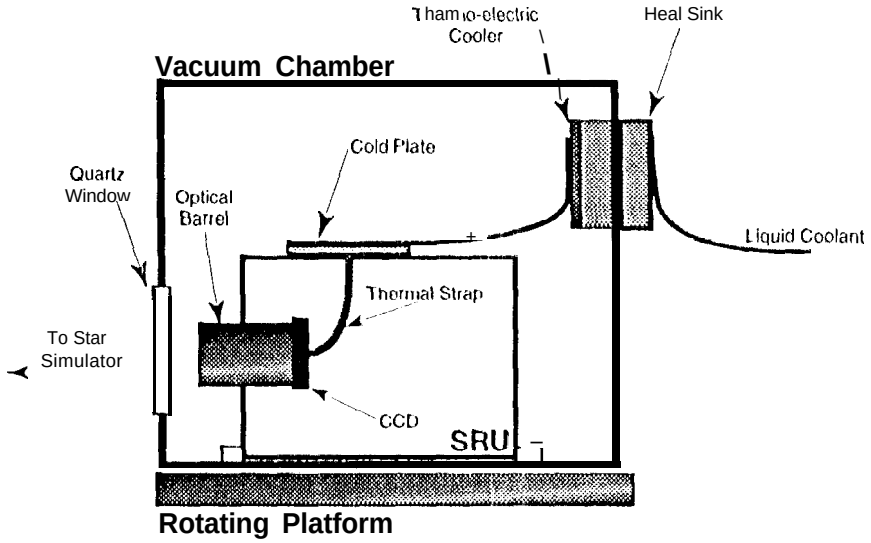

Fig. 3 Vacuum Container Configuration

3.2.2 Accuracy Test Procedures

The accuracy measurements are made to verify:

Centroiding error (lligll spatial frc.clue.l~cy bias erl(~r)	≤ 28 µrad, 3σ
Geometric distortion (low spatial frequency bias error)	≤ 35 µrad, 3σ
Noise Equivalent Angle (NEA)	≤ 47 µrad, 3σ
Total accuracy (RSS of three components)	≤ 65 µrad, 3σ

Centroiding error - Since the required accuracy, 28 µrad, is lcss than the distance that a pixel subtends (approximately 266 µrad), the star spot is intentionally spread over several pixels to allow interpolation of the star position to subpixel level. The interpolatio n error is the difference between the measured centroid position and a straight line transfer function across a pixel domain. A plot of the centroid error would produce a typical " S" curve. The centroiding error is dependent on the spot shape, and therefore 011 the FOV position. The centroiding error is obtained by moving the star across a pixel with 1/30 of a pixel step, and computing the standard deviation of the measured errors at each of the 30 positions. This operation is repeated several times at different points on the FOV (32 to 64 depending on the test phase). The worst standard deviation over the FOV defines the centroid er or.

Distortion error - The distortion of the optics causes the true. angular position of the star in the FOV to be shifted when mapped to the CCD. The distortion error is the difference between the true star position and the measurement. For the SRU, the uncalibrated distortion error is on the order of mrads, therefore a large correction is required to reduce the residual error to within the required 35 µrad. Calibration residual is the RSS of the difference between the. mean values of the interpolation errors (over a pixel as described above) and the actual source position.

NEA - The NEA is the uncertainty in position caused by temporal randomness of the output digital signal due to signal, background and dark current shot noise, detector readout and video amplifier noise. The NEA is found by taking the standard deviation of a large number of measurements performed at a fixed star position. The NEA is a function of the signal-to-noise rat io, and therefore of the star brightness. NEA measurements are made at several locations across the FOV and for several effective star temperatures. The worst value of the NEA measuren ient is used to satisfy the requirement.

3.2.3 Test Results

In the time frame of the Cassini program, three flight model SRUs were manufactured and tested. The first model, FM1, was used for protoflight level environmental testing and will be used as the flight spare. The star spot produced on this model is slightly different from that obtained with the second and third flight models (FM2 and FM3) due to a slightly di fferent focal length achieved during final assembly. An optimized focal length was used cm the later models based on the. test experience with FM1. The performance results described below are from measurements made on FM2 and FM3.

3.2.3.1 Centroiding error

The interp olation error measurements showed that the centroiding error is 20 µrad (3σ) when operating with a 6.0 visual magnitude, G0 star and the CCD cooled to -20 °C. This error becomes 15.5 µrad (3σ) when operating with red stars (producing a higher signal) and is 23.5 µrad (3σ) with blue stars (producing a lower signal). The expected centroiding error, relevant to l)cgirlllir~g-c~f-life conditions, was ≤ 25 µrad (3σ). This accuracy remains unchanged after random vibration (10 g rms) and over the optics temperature range of -15 to +35 °C. Tests performed on FM1, the protoflight model, showed very high stability even for optics temperatures ranging from -35 to + 55 °C.

The expected increase of the. centroiding error at end-of-life is 3 µrad (due.to increasing dark current and reduction of optical transmission). Therefore, the results indicate that the 28 µrad accuracy requirement will be always met.

3.2.3.2 Distortion

The most challenging activity related to performance verification was the calibration of tile optics distortion. An appropriate polynomial function of two variables was defined during the design phase and its acceptability for correcting the distor ion error has been verified during the test phase. Fig. 4 shows the calibration function to be applied for the h coordinate of the two axes. A similar function is obtained for the v-axis. The uncalibrated error, which is on the order of mrads, is reduced to 30 µrad (3σ) after the correction function is applied. This should remain essentially unchanged at end-of-life. The expected residual error after calibration was 27 µrad (3σ).

The residual error also remained unchanged after vibration and pyroshock tests, demonstrating a very good mechanical stability of the optical assembly. Additional tests were performed to verify calibration capability when red and blue stars are used (different chromatic effects induced by the optics). A law describing the focal length variations versus star color has hccn validated, demonstrating that the 30 µrad accuracy can be maintained in the required star spectral range. Finally, perfor mance tests, with the SRU maintained at various temperatures, were used to calibrate focal length versus optics temperature and to verify error stability over the operating temperature range. Results of the the.rllml tests showed that once the focal length is corrected for temperature, the residual distortion error remains unchanged.

For each flight SRU, a set of distortion calibration parameters and star color and optics temperature dependent parameters for focal length correction, are delivered. Use of these parameters in flight will allow the SRU to achieve the same accuracy as measured using the star simulator.

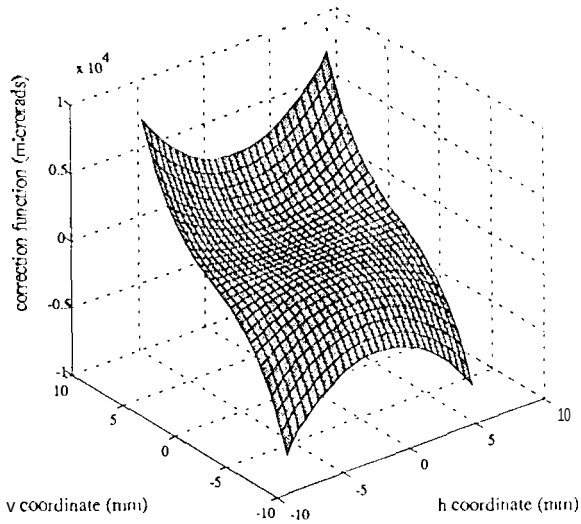

Fig. 4 SRU h-axis Optics Distortion Correction Function

Another interesting way to characterize the. bias error is shown in Fig. 5. In this case., the. global bias error (centroiding plus distortion) in 95% of the measurements showed an error ranging between -3.5 arcsec (-17.5 µrad) and + 5.5 arcsec (27.5 µrad). The maximum error found was 7.2 arcsec (36 µrad).

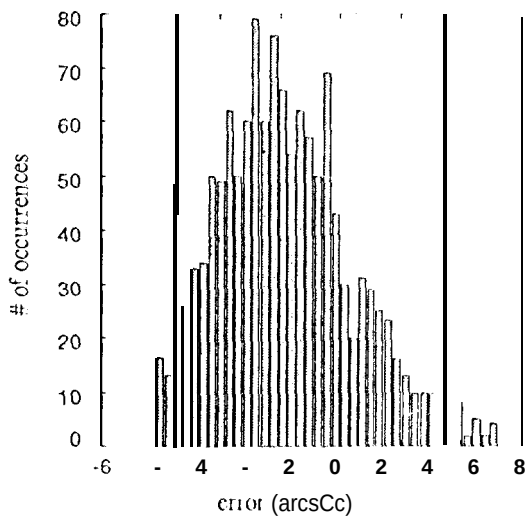

Fig. 5 SRU h-axis Bias Error

3.2.3.3. NEA

1 'ig. 6 reports the expected and measured NEA. As can be seen from this figure, there is a good agreement between experimental and theoretical data for high signal level. A difference of about 7 μrad (3 sigma) is present at lower signals. In any case, it must be considered that the NEA measurement is also affected by the set up stability during the data acquisition. The rotating {able stability during acquisition is twice the encoder resolution (that is 4 μrad). This additional set up noise is introduced in the instrument NEA measurement.

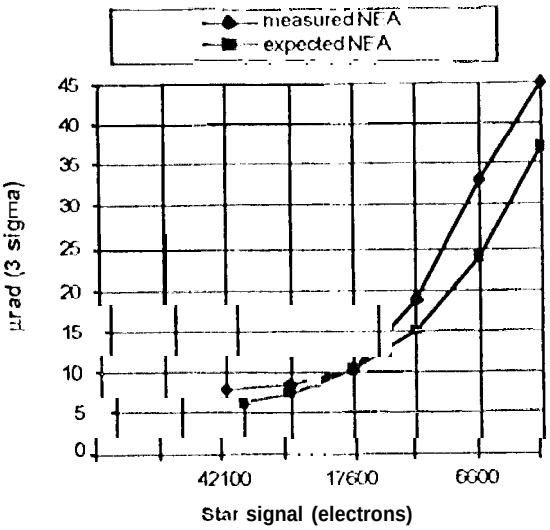

Fig. 6 SRU Noise Equivalent Angle

3.3 SRU Engineering Model Sky Tests

Tests performed with star simulators and precision positioning equipment arc useful for determining the absolute measurement accuracy and stability of the SRU camera assembly. To make these measurements at multiple wavelengths over the range of signal levels representing the different classes of stars used during flight, the star simulator employs a number of spectral and neutral density filters. However, since the performance of these filters is not sufficient to reproduce the actual optical radiation from the various star classes, it is difficult or even impossible to make accurate photometry measurements with the star simulator. To measure the photometric performance of the SRU with real star signals the EM was taken to JPL's Table Mountain Observatory ('I"MC)) from Sept. 24 to Sept. 30, 1995.

The distortions inherent in the SRU optical system, such as distortion as a function of position in the field of view, chromatic distortion duc to different star spectral classes, and changes in focal length from the]-lllrrl changes of the optical barrel are calculated from measurements made with the ASTRA star simulator as described above. These calibration parameters arc then used in the Cassini flight software to correct for the SRU geometric distortion, The 'I" MC) sky data was used to verify that the calculated calibration parameters matched the actual optical performance of the. SRU. In addition, the TMO tests with the. SRU EM provided an opportunity to test the star identification and star tracking algorithms used in the AACS flight software.

3.3.1 TMO Test Set-Up

Table Mountain Observatory has been used as a test site for J] 'l, star trackers and sun sensors for a number of years. Located near Wrightwood California, at an altitude of 7500 feet, TMO maintains and operates several astronomical telescopes. For the SRU sky tests, the EM was mounted "piggyback" on the 24" Schmitt-Cassegrain telescope. The pointing and tracking system of the telescope enabled the test operator to point the SRU optical boresight at different areas of the sky containing stars of various magnitudes and spectral classes. The telescope optics were not used during these tests.

The SRU is controlled in flight by the AEC and the SRU Manager module of AACS flight software. For testing at 'I'MC), a VME based computer system, with custom interface boards simulating the Bus Controller Input/Output Unit (BCIOU) and Pixel Input Unit (PIU) circuits of the flight computer, was used to control the SRU and to collect the pixel

data. These circuits provide the same electrical interface and data protocol as the flight computer circuits. The VME computer was connected via ethernet to a Sun workstation where the test software was developed and the test data was stored.

3.3.2 Test Procedure

The apparent visual brightness of a star, or its visual magnitude, M_{vis}, is specified by a logarithmic scale based on human visual perception. This visual magnitude is the reference value that is included in most star catalogs. The CCD sensor in the SRU, however, has a spectral response that is different from the human visual response. The peak response of the CCD is at a longer wavelength than the eye's peak response. One of the objectives of the sky tests, in conjunction with the simulations, is to develop a magnitude correction factor for a set of star spectral classes that can be used for calculating an instrument magnitude for each star in the. on-board catalog. This SRU instrument magnitude is then used during the mission by the attitude initialization software as one of the criteria for identifying stars and for matching stars during tracking. The determination of the instrument magnitude, is made by collecting a large number of SRU star field images, identifying the stars in the field, measuring the signal level of the stars, and then correlating the difference between the measured brightness of the stars and the cataloged brightness value to a color parameter of the star. The parameter typically used is the B-V color index.

3.3.3 Test Results

A large number of SRU star field images were collected over several observing nights at "I'M(). The flight software star identification algorithms were used to identify stars in the images and calculate the pointing direction, in terms of sky coordinates, of the SRU optical boresight. Test software then re-scanned the images and extracted additional stars from the field of view (stars not used for determining the pointing direction) and determined the stars' magnitude and spectral data from a star catalog. The signal levels of the stars, as measured by the SRU, were normalized to account for differences in exposure times between the images. The instrument magnitude of each star was then determined using these normalized signal levels. The difference of this instrument magnitude from the visual magnitude from the star catalog versus the B-V color index was found to be

$$M_{ins} = M_{vis} - 0.59(1! - V). \quad (1)$$

This parameter will be included as an entry in the on-board star catalog 10 compensate for the spectral response of the SRU. A plot of the magnitude **diffcrcncc** versus B-V, based on measurements of about 1200 stars, is shown in Fig. '?. This equation provides a good correction of the instrument magnitude over the stellar spectral classes that are used during flight.

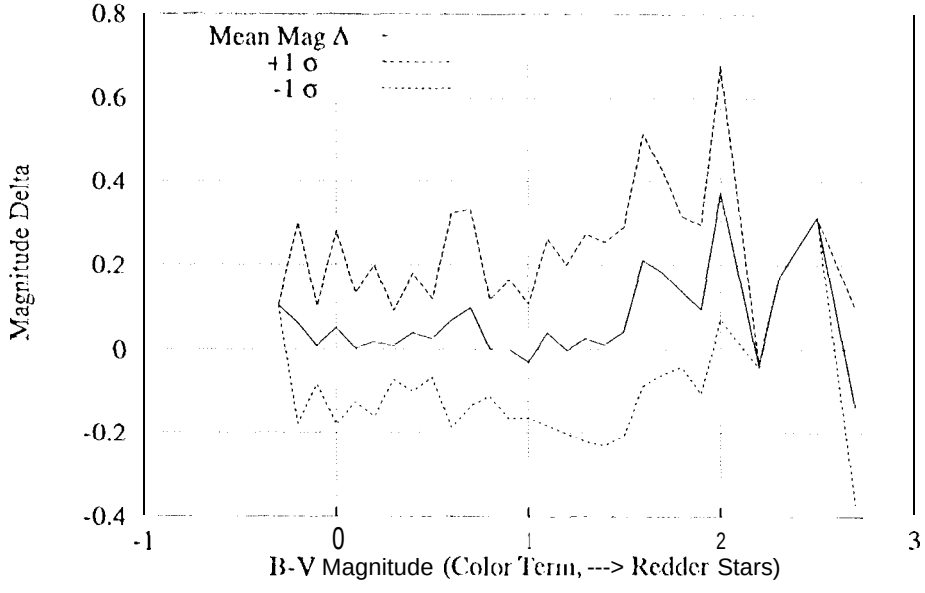

Fig. 7 SRU Magnitude Delta versus B-V

The stat catalog listings for the identified stars also include very accurate measurements of the star positions in sky coordinates. These catalog positions were compared with the SRU measured positions 10 determine the capability of the optical calibration parameters to compensate for distortion in the SRU optics. One of the principal contributions to the optical distortion is spherical aberration. This distortion would cause star images near the edge of the SRU field of view to have a g; cater measurement error than images close to the optical boresight. One convenient way to interpret these radial errors is to characterize. them as a change in optical focal length as a function of (hc radial distance from the center of the field of view. A plot of this effect is shown in Fig. 8.

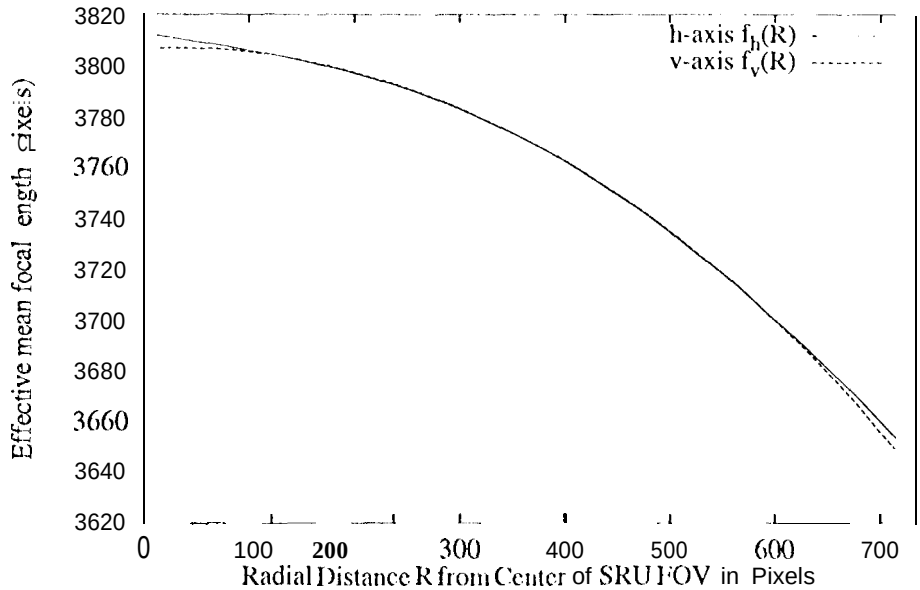

Fig. 8 Mean SRU Focal Length versus Radial Distance from Center of the FOV

1 'or the tests performed at 'I"MO, the application of the radial compensation term alone, ignoring non-radial optical distor tion and distortions duc to thermal and chromatic effects, was sufficient to bring the measurement errors due. to optical distortion below the level needed to meet the required measurement accuracy specification of the SRU.

4. IMAGE EMULATION '1'11S'1' APPROACH

The SRU is controlled in flight by the AACS flight computer running software that reads the CCD pixel data and calculates the positions of stars in the SRU field of view. These star positions arc then used to determine the current attitude of the spacecraft and to estimate the attitude change for the next SRU measurement cycle. The SRU manage.r software uses the altitude predictions to reposition the SRU readout windows to insure that the stars being tracked arc kept within the window boundaries on the next measurement cycle. It is difficult 10 exhaustively test the possible interactions between the SRU manager software and the attitude estimator software running in the AFC and between the software and the SRU hardware without a complete set of star data from all conceivable pointing directions in the sky. Traditional tests of attitude control systems, with an artificial optical stimulus for the star tracker as an example, cannot produce a sufficiently high fidelity simulation of the complete closed loop system to provide confidence in the integrity of the software. To facilitate a closed loop simulation of the flight software, the SRU contains a dedicated hardware interface that allows a direct injection of simulated fields of view into the SRU and subsequently into the pixel input buffers in the AFC. These simulated pixels replace the pixels read from the CCD and processed by the SRU analog signal circuits. Since these synthetic pixel values can be generated to resemble real sky data, this test approach allows the SRU to output pixels to the AFC memory which emulate star fields that would bc imaged in flight. This SRU hardware inter face is connected to a custom designed bow-d in the AACS Support Equipment (SE). The boat d stores the synthetic pixel data in a block of memory until it is accessed by the SRU. This board, along with the VME computer that generates the synthetic pixels, is known as the Image Emulation Unit.

The Image simulation Unit (IEU) consists of three main components: a VME based array processor computer, a block of static RAM with the necessary interface circuits, and interface circuits that enable the transfer of the pixels into the SRU. The IEU processor includes a connection to the AACS SE which enables the IEU software to produce a high quality reproduction of a star field that would be imaged during flight. This SE interface provides the IEU software with the simulated pointing direction of the SRU boresight and the SRU hardware configuration, i.e. window positions, exposure time, gain setting, etc. The IEU software locates the stars that would be visible in the SRU field of view at the simulated attitude in a star catalog, generates the pixel values that would be generated on the CCD from the incident star signals, adjusts the pixel values to match the SRU configuration, and finally stores the synthetic pixels in the IEU memory buffer. A complete description of the IEU software and its interactions with the SE software is provided in an accompanying paper by J. Alexander and D. Chang.[3]

The IEU memory buffer is a two megabyte block of static ram capable of storing onc complete CCD image. This buffer is coupled to the IEU processor through a dedicated VME Subsystem Bus (VSB) which prevents any other processes that may be occurring in the IEU chassis from interfering with pixel transfers. The pixel values in the IEU memory buffer are transmitted to the SRU through a set of twelve parallel, isolated, differential signal drivers.

The IEU/SRU link consists of the twelve pixel signals, timing signals from the SRU, and a control line that allows the SRU electronics to detect if the IEU connection is present. The control of these signals, along with the VSB bus interface signals, is achieve.d by digital circuits implemented in a custom dc.signed field programmable gate array. The SRU timing signals cause the IEU memory buffer address to be incremented for every SRU pixel that would be processed if the data from the CCD were being read. These SRU generated signals insure that the timing of the pixel transfers to the AFC memory is identical to the timing that would be seen in flight. The remaining control signal from the IEU specifics to the SRU that the IEU is connected and that the pixel path from the analog circuits should be interrupted and that IEU pixels should sent to the AFC in place of CCD pixels. Disabling this signal removes power from the. IEU interface circuits in the. SRU. The SRU connector that contains this signal, and all of the IEU signals, is not used in flight and therefore the. possibility of intern option of the CCD pixels in flight is eliminated.

The IEU has been used extensively for development of the flight software star identification and tracking algorithms. The ability to simulate star field images from the SRU and simultaneously access the actual flight hardware interfaces has enabled the entire software to be tested as a unit instead of separate modules that later would need to be integrated together. In addition, the IEU can be used to introduce faults into the SRU output data, such as increased noise levels, high background signals, or damage to the. CCD from radiation. The response. of the AACS fault protection software to these conditions can be tested in a way that would not be possible without the IEU. The IEU has been shown to be a very valuable tool in the development, verification and integration of the Cassini attitude control system.

s. SUMMARY

The results of an extensive and robust SRU test program have shown that the SRU will behave predictably and reliably during the harsh journey to and exploration of the Saturnian system. The combined effort of JPL and OG has produced volumes of performance data that verifies that the SRU performance specifications will be met. Two flight SRUs have been successfully integrated on the Cassini spacecraft which is undergoing preparations for system level environmental testing. The EM and the flight spare SRU will continue to be used to support AACS subsystem level testing in the AACS Integrated Test Lab (ITL) through launch and during mission operations.

6. ACKNOWLEDGMENTS

The authors would like to thank Ed Dennison for his assistance during the sky tests at 'Table Mountain Observatory and Jim Alexander for his help with the data analysis. Chris Clark deserves special kudos for the long hours spent testing CCDs.

The research described in this paper was carried out by the Jet Propulsion Laboratory, California Institute of Technology, under a contract with the National Aeronautics and Space Administration.

7. REFERENCES

1. V. C. Thomas, J. W. Alexander, E. W Dennison and T. Waddell, "Cassini star tracking and identification architecture," *Proc. SPIE*, vol. 2221, pp. 15-26, 1994.

2. G. Borghi, D. Procopio, M. Magnani, S. Pieri, S. Becucci, "Stellar Reference Unit for Cassini Mission," *Proc. SPIE*, vol. 2210, pp. 150-161, 1994.
3. J. W. Alexander and D. H. Chang, "Cassini star tracking and identification algorithms, scene simulation, and testing," *Proc. SPIE*, Vol. 2803, 1996.